Nanoelectromechanical Switches by Controlled Switchable Cracking

Qiang Luo, Zhe Guo, Houbing Huang, Qiming Zou, Xiangwei Jiang, Shuai Zhang, Hongjuan Wang, Min Song, Bao Zhang, Hong Chen, Haoshuang Gu, Genquan Han, Xiaofei Yang, Xuecheng Zou, Kai-You Wang, Zhiqi Liu, Jeongmin Hong, Ramamoorthy Ramesh, and Long You, *Member, IEEE*

***Abstract*— Nanoelectromechanical (NEM) switches could surmount the Boltzmann Tyranny in the current charge-carrier systems. However, thus far, practical implementations of the NEM systems have been hindered by the complicated fabrication processes of forming the extremely small air gap. Here, we realize a very simple NEM switch by exploiting a switchable nanocrack controlled by an electric field in a metallic alloy-ferroelectric heterostructure. The crack is formed in a controllable manner in terms of its initiation, location, and orientation through a bridge-like structure. The open and closed states of the crack are programmed under a cyclic electric field. In addition, an abrupt switching behavior with a nonvolatile high ON/OFF current ratio ($>10^7$) is measured owing to the near-zero OFF-state leakage current across the crack. This simple nanocrack switch presents a novel opportunity in the NEM systems, which can be used as a new nonvolatile random-access memory and logic.**

***Index Terms*— Nanoelectromechanical switch, controlled nanocrack, electric field control, nonvolatile memory.**

Manuscript received April 22, 2019; revised May 7, 2019, May 13, 2019 and May 16, 2019; accepted May 16, 2019. Date of publication May 21, 2019; date of current version June 26, 2019. This work was supported by the National Natural Science Foundation of China under Grant 61674062 and Grant 61821003. The review of this letter was arranged by Editor E. A. Gutiérrez-D. *(Qiang Luo and Zhe Guo contributed equally to this work.) (Corresponding author: Long You.)*

Q. Luo, Z. Guo, S. Zhang, X. Yang, X. Zou, J. Hong, and L. You are with the School of Optical and Electronic Information, Huazhong University of Science and Technology, Wuhan 430074, China (e-mail: lyou@hust.edu.cn).

H. Huang is with the Advanced Research Institute of Multidisciplinary Science, Beijing Institute of Technology, Beijing 100081, China.

Q. Zou is with the Department of Electrical and Computer Engineering, University of Nebraska-Lincoln, Lincoln, NE 68588 USA.

X. Jiang, B. Zhang, and K.-Y. Wang are with the State Key Laboratory for Superlattices and Microstructures, Institute of Semiconductors, University of Chinese Academy of Sciences, Beijing 100083, China.

H. Wang is with the State Key Laboratory for Superlattices and Microstructures, Institute of Semiconductors, University of Chinese Academy of Sciences, Beijing 100083, China, and also with the School of Microelectronics, Xidian University, Xi'an 710071, China.

M. Song and H. Gu are with the Hubei Key Laboratory of Ferro and Piezoelectric Materials and Devices, Faculty of Physics and Electronic Science, Hubei University, Wuhan 430062, China.

G. Han is with the School of Microelectronics, Xidian University, Xi'an 710071, China.

H. Chen is with School of Materials Science and Energy Engineering, Foshan University, Foshan 528000, China.

Z. Liu is with the School of Materials Science and Engineering, Beihang University, Beijing 100191, China.

R. Ramesh is with the Department of Materials Science and Engineering, University of California at Berkeley, Berkeley, CA 94720 USA.

Color versions of one or more of the figures in this letter are available online at http://ieeexplore.ieee.org.

Digital Object Identifier 10.1109/LED.2019.2917924

I. Introduction

CRACKS are generally considered as defects in electronic devices. However, many intriguing crack-based structures and devices have been demonstrated, such as ultrasensitive mechanical sensors [1]–[3], high-resolution patterning [4]–[6], and electronic nanogaps [7]–[8]. Most of these utilized the "micro-notch" structures and confined surface stress to form the cracks in thin brittle materials [2]–[10]. Recently, another new type of cracks in a metallic alloy-ferroelectric heterostructure, which can open or close reversibly under electric field, has been reported [11]–[12]. The reversible opening and closing of the cracks can induce a huge resistance change in the alloy film, illustrating the potential for the future memory or logic. Nevertheless, it is hindered by the random distribution of cracks throughout the structure, which is the main obstacle to actual application. Critically, the precise control of nanocracking is the key factor for a variety of applications [4]–[7], [10].

The mechanical switching process of the crack with nanoscale width resembles the nanoelectromechanical (NEM) switch, which operates by nanometer-scale motion to make and break physical contact between electrodes and hence do not rely on energy-barrier modulation as the switching mechanism [13]–[17]. Here, we demonstrate the direct control of location, orientation and electrical switching of nanocrack, by using a "bridge-like" structure in the alloy film-ferroelectric heterostructure. Based on such structure, a novel NEM switch with easy fabrication process, high on/off ratio, and low power consumption is also proposed.

II. Crack-Based NEM Switch Concept

Our device consists of a conductive alloy thin film grown on top of a ferroelectric substrate. The conductive thin film is patterned to outline a bridge-like structure as illustrated in Fig. 1a. Next, the crack-forming process is conducted through by applying a cyclic electric field along the thickness direction of the substrate. Then, the crack initiates at the edge of the active area and is oriented in the width direction (the crack location is discussed in detail later). More importantly, the crack state (open or closed) can also be controlled by the electric field. A negative electric field results in the opening of the crack (Fig. 1b), whereas a positive one can lead to the closed state (Fig. 1c). Accordingly, the opening and closing of the crack can break and connect the current path in the alloy film, constructing a NEM switch.

We demonstrate such a crack-based NEM switch using a $Mn_{50}Pt_{50}$ alloy film and (001)-oriented PMN-PT single-crystal substrate. $Mn_{50}Pt_{50}$ was chosen because of its intermediate

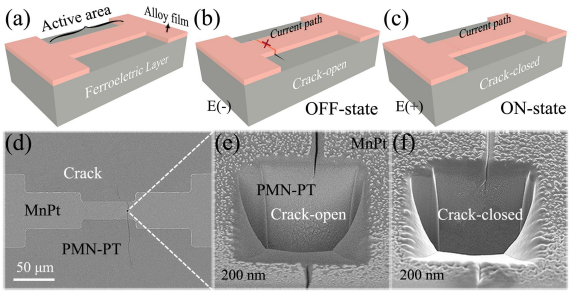

Fig. 1. (a) Schematic of the device, which consists of a bridge-like patterned alloy thin film and ferroelectric substrate. (b) Open state of the crack under a negative electric field. The current path in the alloy thin film is broken by the open crack. (c) Closed state under a positive electric field. The corresponding current path is connected. The cross-section SEM images of the (e) open state and (f) closed state of the crack at the same location (d) are based on the PMN-PT/MnPt heterostructure controlled by an electric field. The dashed squares in (e) and (f) represent the FIB etched window.

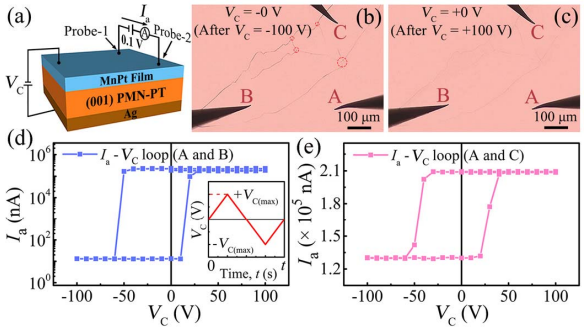

Fig. 2. (a) Schematic of the heterostructure without patterning and two-probe resistance measurement setup. The positive direction of V_C is defined from the bottom to the top electrode. (b) and (c) show the partial optical microscopy images of the cracks in the macroscopic thin film after scanning V_C from (b) −100 V and (c) +100 V to 0 V, where the points A, B and C represent different probe locations for measurement. (d) and (e) show the current I_a as a function of V_C collected from two probes located at (d) points A and B and (e) points A and C, respectively. Inset shows electrical waveform for both generating and manipulating the cracks. Notice that (d) and (e) show different on/off ratios.

mechanical properties, which are very close to the empirical boundary between ductile and brittle materials [12]. To clearly observe the configuration of the NEM switch, cross-section scanning electron microscope (SEM) images of the crack in different states (Fig. 1e and f) were acquired using a focused ion beam (FIB). It is clear that the crack extends from PMN-PT into the MnPt film, which forms a metal-metal nano-gap in the film. The actuation of conventional NEM switches includes a variety of methods, for example, electrostatic, thermal, piezoelectric and resonant switching [13]. However, the top-down approach for fabrication requires complicated processing steps involving electronic beam lithography, nanomachining and coating technologies. By contrast, here, the manipulation of a controlled crack by an electric field enables the development of a new simple approach for the implementation of NEM switches.

III. Voltage Control of Cracks in Thin Films

Firstly, we investigated the properties of cracks generated in a macroscopic MnPt thin film. As shown in Fig. 2a, a 40-nm MnPt film was deposited on a PMN-PT substrate (5 mm × 5 mm × 0.5 mm) at room temperature by magnetron sputtering. Then a triangular voltage V_C (inset in Fig. 2d) up to 300 V with a period of t = 4 min was applied between the top MnPt film and the bottom Ag electrode to induce cracks. After the forming process, the crack states (open or closed) were manipulated under V_C up to 100 V (larger than the switching field) with t = 80 s. When V_C varied from −100 to 0 V, the cracks were distinctly visible by optical microscopy (Fig. 2b), indicating the open state of the cracks. However, virtually all the cracks disappeared after scanning V_C from +100 to 0 V (Fig. 2c). The optical images show that multiple cracks are generated in the MnPt film after a single application of the electric field, and that the cracks are distributed randomly. In addition, the generated cracks intersect with boundaries or with each other (indicated by the dashed circle in Fig. 2b), complicating the morphology of the cracks.

Then the electrical performance of the cracks was measured through a two-probe resistance measurement (Fig. 2a). The current I_a was measured when a constant voltage of 0.1 V was applied between the two probes. Fig. 2d shows one of the results, which was collected from the two probes located at A and B as labeled in Fig. 2b. A positive V_C higher than 25 V induces a high I_a of approximately 0.1 mA, while I_a is reduced to 10 nA under negative V_C lower than −60 V, resulting in a decline in I_a of four orders of magnitude. When we measured the result between the probes at points A and C, a similar square-like loop was observed; however, the variation in I_a was several orders of magnitude smaller. On sweeping V_C from −100 to 100 V, I_a varies from just 0.13 to 0.21 mA (Fig. 2e). The different I_a variations between the two results are associated with the random distribution of the cracks in the film. Here, test point B is surrounded by cracks. Thus, when those cracks are open, very little current can flow between A and B, and thereby a low value of I_a is observed. However, A and C are not separated completely by the cracks, and electrical percolation still exists between these two points, even when the cracks are open. This results in only a small decrease in I_a.

From these results, it can be found that the electrical performance of the cracks in the macroscopic film strongly depends on the test point positions, which is attributed to the random distribution of the cracks. Therefore, further precise control of crack is urgently required for actual applications.

IV. Precise Control of Crack

Next, we used photolithography followed by etching to pattern the bridge-like structure. Fig. 3a shows the schematic of the patterned device and the measurement setup.

The method for generating a crack in the bridge-like device is similar to that in the film. At the end of each V_C cycle (inset in Fig. 2d), the maximum of V_C ($V_{C(max)}$) gradually increased in 10 V intervals until the crack was induced. In our experiment, when $V_{C(max)}$ reached 130 V, a crack was generated at the edge of the active area and propagated across the width of the bridge structure. Fig. 3b shows the nonvolatile open state of the generated nanocrack (∼50-nm width) when V_C was varied from −100 to 0 V, whereas the closed state is shown in Fig. 3c. Accordingly, I_a (device 1) decreased sharply from ∼150 μA to near zero upon applying the negative V_C with a magnitude of −65 V, and I_a reached ∼0.4 pA when V_C recovered back to 0 V, as indicated by arrows 1 and 2 in Fig. 3d. Symmetrically, voltages of approximately +65 V switched I_a from 10 pA to the saturated value, and I_a was

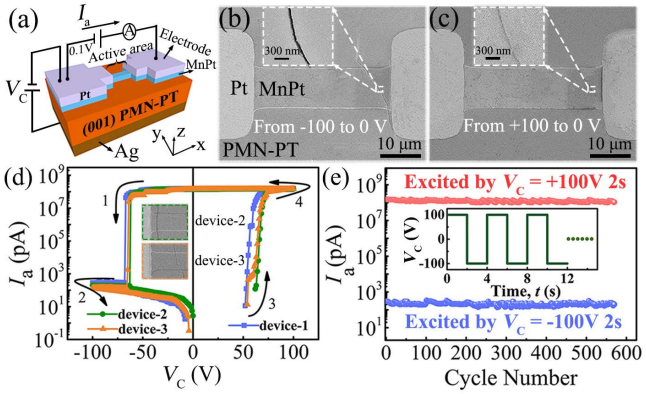

Fig. 3. (a) Schematic of the device with the bridge-like structure and the corresponding resistance measurement setup. (b) and (c) show the top-view SEM images of the active area with the (b) open and (c) closed state of the crack. (d) The current I_a as a function of V_C collected from different devices. The insets show the SEM images of other two devices. The voltage step and time interval of V_C were fixed at 1 V and 1 s, respectively. (e) Repeatability test for the switching of crack via voltage pulses (the inset shows the pulse details). The amplitude and duration of the pulse were 100 V and 2 s, respectively.

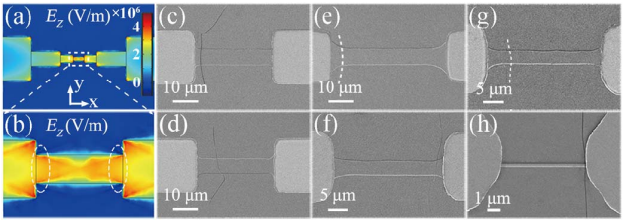

Fig. 4. (a) Top-view E_Z distribution in the bridge-like structure using COMSOL Multiphysics simulation. (b) The enlarged view for the active area. The cracks induced by electric field in devices with different active area sizes (c) 6 μm × 30 μm, (d) 5 μm × 30 μm, (e) 7 μm × 40 μm, (f) 3.5 μm × 30 μm, (g) 3 μm × 30 μm, (h) 0.3 μm × 6.5 μm. The dashed lines in (e) and (g) are used to indicate the crack.

unchanged as V_C was swept from +100 to 0 V, as represented by arrows 3 and 4 in Fig. 3d. The *I-V* characteristics of the other two devices (same size as the device 1) are also demonstrated in Fig. 3d, showing similar square loops.

A repeatability test was also performed, as shown in Fig. 3e. Alternating voltages of ±100 V with a time interval of 2 s were applied, and I_a was measured during voltage application. The positive voltage results in high I_a values (represented by red dots), while the negative voltage induces low I_a values (indicated by blue dots). Neither the high nor the low values of I_a changed greatly during the several hundred tests. However, the crack did not close completely with increasing cycling times, resulting in an increase in ON contact resistance and failure of the device. We attribute this to the contact contamination and the uneven contact surface of the crack. To further improve the reliability, a contact material with suitable mechanical properties and high robustness to the surface contamination, such as oxidation, hydrocarbon and tribopolymer formation, can be employed in the device [18]. Moreover, a ferroelectric layer with a regular domain structure can be used to form the smooth crack surface for reliability optimization.

With such a patterned structure, the crack location can be confined within certain regions, despite the random distribution of cracks in the macroscopic thin film. The crack orientation was also along the specific direction.

Now, we briefly discuss the mechanism of switching of the crack to understand the reason for realizing such precise control. The applied electric fields switch the ferroelectric domain and produce a large strain at the domain boundary. The crack is induced to relax the severe increase in elastic energy, which also introduces additional surface energy. Therefore, the crack forms easily in zones in which the ferroelectric domain switching occurs more easily, or in other words, those with higher electric field distributions. After the forming process, the switching of the crack under electric field is governed mainly by the competition between the electromechanical-strain-related elastic energy and the surface energy [12]. In addition, owing to the nonvolatile switching of the 109° domain in the PMN-PT, the switching of the crack also exhibits the nonvolatility [19].

Hence, we analyzed the electric-field distribution in our bridge-like device. Fig. 4a shows the z-component distribution of the perpendicularly applied electric field (E_Z) in the device; this is the main factor determining the domain switching. It is clear that the distribution of E_Z is not uniform in the patterned device. In fact, the highest values of E_Z are distributed mainly at the corners, as indicated by the red zones in Fig. 4a. In particular, in the active area, the highest values of E_Z are distributed at the edges, as indicated by the dashed circle in Fig. 4b, and the distributions of E_Z are axisymmetric relative to the x-axis. Critically the crack generated in our fabricated device shown in Fig. 3b and 3c is located exactly in this zone and is oriented along the width of the bridge structure. Moreover, the cracks generated in other devices of different sizes (Fig. 4c-h) are also located in the same or similar zone(s). The excellent agreement between the theoretical simulation and the experimental observation confirms the feasibility of our method.

The resistance change in our device is achieved by the voltage (corresponding to a small electric field of ~1.3 kV/cm) applied to the highly insulating ferroelectric substrate, and the Joule heating is negligible. As a result, the switching energy can be ultralow once such a device is scaled down to the nanoscale. The writing energy comprises two parts: one is for switching the polarization and the other for the additional surface energy. The ferroelectric polarization switching energy can be estimated using $P_rSV/2$ (P_r is the remnant polarization, S is the cell area and V is the switching voltage) [20] and the surface energy can be calculated as γ A (γ is the surface energy density and A is the surface area) [12]. For a PMN-PT film with a thickness of 2 μm, the switching voltage can be reduced dramatically to 1.3 kV/cm × 2 μm = 0.26 V. Considering a scaled-down active area with a size of 100 nm (length) × 50 nm (width) × 25 nm (thickness of the MnPt film plus crack depth in the PMN-PT film), the calculated total writing energy per bit is 2.695 fJ.

V. Conclusion

The precise control of the nanocrack including the location, orientation, and electrical switching has been demonstrated in the PMN-PT/MnPt heterostructure. Based on such the switchable nanocrack, the NEM switch with a simple fabrication process is also proposed. The crack-based NEM switch will not only provide new opportunities for the nonvolatile memory and logic, but also revolutionize the development of novel multifunctional sensors and IoT products.

REFERENCES

[1] D. Kang, P. V. Pikhitsa, Y. W. Choi, C. Lee, S. S. Shin, L. Piao, B. Park, K.-Y. Suh, T.-I. Kim, and M. Choi, "Ultrasensitive mechanical crack-based sensor inspired by the spider sensory system," *Nature*, vol. 516, pp. 222–226, Dec. 2014. doi: 10.1038/nature14002.

[2] Y. W. Choi, D. Kang, P. V. Pikhitsa, T. Lee, S. M. Kim, G. Lee, D. Tahk, and M. Choi, "Ultra-sensitive pressure sensor based on guided straight mechanical cracks," *Sci. Rep.*, vol. 7, p. 40116, Jan. 2017. doi: 10.1038/srep40116.

[3] M. Amjadi, M. Turan, C. P. Clementson, and M. Sitti, "Parallel Microcracks-based ultrasensitive and highly stretchable strain sensors," *ACS Appl. Mater. Interfaces*, vol. 8, no. 8, pp. 5618–5626, Feb. 2016. doi: 10.1021/acsami.5b12588.

[4] K. H. Nam, I. H. Park, and S. H. Ko, "Patterning by controlled cracking," *Nature*, vol. 485, no. 7397, pp. 221–224, May 2012. doi: 10.1038/nature11002.

[5] M. Kim, D. Ha, and T. Kim, "Cracking-assisted photolithography for mixed-scale patterning and nanofluidic applications," *Nature Commun.*, vol. 6, Feb. 2015, Art. no. 6247. doi: 10.1038/ncomms7247.

[6] B. C. Kim, T. Matsuoka, C. Moraes, J. Huang, M. D. Thouless, and S. Takayama, "Guided fracture of films on soft substrates to create micro/nano-feature arrays with controlled periodicity," *Sci. Rep.*, vol. 3, Oct. 2013, Art. no. 3027. doi: 10.1038/srep03027.

[7] V. Dubois, F. Niklaus, and G. Stemme, "Crack-defined electronic nanogaps," *Adv. Mater.*, vol. 28, pp. 2178–2182, Mar. 2016. doi: 10.1002/adma.201504569.

[8] R. Pan, Y. Yang, Y. Wang, S. Li, Z. Liu, Y. Su, B. Quan, Y. Li, C. Gu, and J. Li, "Nanocracking and metallization doubly defined large-scale 3D plasmonic sub-10 nm-gap arrays as extremely sensitive SERS substrates," *Nanoscale*, vol. 10, no. 7, pp. 3171–3180, Feb. 2018. doi: 10.1039/c7nr08646f.

[9] H. Vandeparre, Q. Liu, I. R. Minev, Z. Suo, and S. P. Lacour, "Localization of folds and cracks in thin metal films coated on flexible elastomer foams," *Adv. Mater.*, vol. 25, no. 22, pp. 3117–3121, Apr. 2013. doi: 10.1002/adma.201300587.

[10] J. Shim, S.-H. Bae, W. Kong, D. Lee, K. Qiao, D. Nezich, Y. J. Park, R. Zhao, S. Sundaram, X. Li, H. Yeon, C. Choi, H. Kum, R. Yue, G. Zhou, Y. Ou, K. Lee, J. Moodera, X. Zhao, J.-H. Ahn, C. Hinkle, A. Ougazzaden, and J. Kim, "Controlled crack propagation for atomic precision handling of wafer-scale two-dimensional materials," *Science*, vol. 362, no. 6415, pp. 665–670, Nov. 2018. doi: 10.1126/science.aat8126.

[11] P. Gao, C. T. Nelson, J. R. Jokisaari, S.-H. Baek, C. W. Bark, Y. Zhang, E. Wang, D. G. Schlom, C.-B. Eom, and X. Pan, "Revealing the role of defects in ferroelectric switching with atomic resolution," *Nature Commun.*, vol. 2, Dec. 2011, Art. no. 591. doi: 10.1038/ncomms1600.

[12] Z. Q. Liu, J. H. Liu, M. D. Biegalski, J.-M. Hu, S. L. Shang, Y. Ji, J. M. Wang, S. L. Hsu, A. T. Wong, M. J. Cordill, B. C. Marker, H. Yan, Z. X. Feng, L. You, M. W. Lin, T. Z. Ward, Z. K. Liu, C. B. Jiang, L. Q. Chen, R. O. Ritchie, H. M. Christen, and R. Ramesh, "Electrically reversible cracks in an intermetallic film controlled by an electric field," *Nature Commun.*, vol. 9, p. 41, Jan. 2018. doi: 10.1038/s41467-017-02454-8.

[13] L. Jasulaneca, J. Kosmaca, R. Meija, J. Andzane, and D. Erts, "Electrostatically actuated nanobeam-based nanoelectromechanical switches—Materials solutions and operational conditions," *Beilstein J. Nanotechnol.*, vol. 9, no. 1, pp. 271–300, Jan. 2018. doi: 10.3762/bjnano.9.29.

[14] C. Qian, A. Peschot, B. Osoba, Z. A. Ye, and T.-J. K. Liu, "Sub-100 mV computing with electro-mechanical relays," *IEEE Trans. Electron Devices.*, vol. 63, no. 3, pp. 1315–1321, Mar. 2017. doi: 10.1109/TED.2017.2657554.

[15] U. Zaghloul and G. Piazza, "Sub-1-volt piezoelectric nanoelectromechanical relays with millivolt switching capability," *IEEE Electron Device Lett.*, vol. 35, no. 6, Jun. 2014. doi: 10.1109/LED.2014.2318049.

[16] J. O. Lee, Y.-H. Song, M.-W. Kim, M.-H. Kang, J.-S. Oh, H.-H. Yang, and J.-B. Yoon, "A sub-1-volt nanoelectromechanical switching device," *Nature Nanotech.*, vol. 8, no. 1, pp. 36–40, Jan. 2013. doi: 10.1038/NNANO.2012.208.

[17] T. H. Lee, S. Bhunia, and M. Mehregany, "Electromechanical computing at 500 °C with silicon carbide," *Science*, vol. 329, no. 5997, pp. 1316–1318, Sep. 2010. doi: 10.1126/science.1192511.

[18] O. Changho and B. M. P. de, "Contact reliability of Pt- and TiN-coated microswitches in different environments," in *Mechanics of Biological Systems & Micro-and Nanomechanics*, vol. 4. Cham, Switzerland: Springer, 2018, pp. 101–103. doi: 10.1007/978-3-319-95062-4_22.

[19] S. Zhang, Y. G. Zhao, P. S. Li, J. J. Yang, S. Rizwan, J. X. Zhang, J. Seidel, T. L. Qu, Y. J. Yang, Z. L. Luo, Q. He, T. Zou, Q. P. Chen, J. W. Wang, L. F. Yang, Y. Sun, Y. Z. Wu, X. Xiao, X. F. Jin, J. Huang, C. Gao, and X. F. R. Han nad Ramesh, "Electric-field control of nonvolatile magnetization in Co40Fe40B20/Pb(Mg1/3Nb2/3)0.7Ti0.3O3 Structure at room temperature," *Phys. Rev. Lett.*, vol. 108, no. 13, Mar. 2012, Art. no. 137203. doi: 10.1103/PhysRevLett.108.137203.

[20] J. M. Hu, Z. Li, L. Q. Chen, and C. W. Nan, "High-density magnetoresistive random access memory operating at ultralow voltage at room temperature," *Nature Commun.*, vol. 2, p. 553, Nov. 2011. doi: 10.1038/ncomms1564.